

Vibrational energy transfer between CO and CH₄, CD₄, and CF₄ in liquid Ar

Hamzeh AbdelHalim and George E. Ewing

Citation: *The Journal of Chemical Physics* **82**, 5442 (1985); doi: 10.1063/1.448578

View online: <http://dx.doi.org/10.1063/1.448578>

View Table of Contents: <http://scitation.aip.org/content/aip/journal/jcp/82/12?ver=pdfcov>

Published by the AIP Publishing

Articles you may be interested in

[Collisional energy transfer between Ar and normal and vibrationally and rotationally frozen internally excited benzene-trajectory calculations](#)

J. Chem. Phys. **106**, 7080 (1997); 10.1063/1.473730

[Vibrational energy transfer between isotopes of CO and isotopes of CO₂ in the gas phase and in liquid Kr solution](#)

J. Chem. Phys. **102**, 1192 (1995); 10.1063/1.468906

[Pure vibrational Raman spectra of simple liquids: O₂, N₂, CO, CH₄, CF₄](#)

J. Chem. Phys. **73**, 673 (1980); 10.1063/1.440169

[Vibrational energy transfer rates for the CO–CH₄, CO–CF₄, and CO–SF₆ systems](#)

J. Chem. Phys. **63**, 2242 (1975); 10.1063/1.431608

[Vibrational Energy Transfer between CO and COS: A Test of the Harmonic Oscillator Model](#)

J. Chem. Phys. **57**, 3575 (1972); 10.1063/1.1678797



Vibrational energy transfer between CO and CH₄, CD₄, and CF₄ in liquid Ar^{a)}

Hamzeh Abdel-Halim and George E. Ewing

Department of Chemistry, Indiana University, Bloomington, Indiana 47405

(Received 8 November 1984; accepted 15 March 1985)

Vibrational relaxation of CO ($\nu = 1$) by CH₄, CD₄, and CF₄ in liquid Ar at 87 K has been studied. The IR fluorescence decay from CO ($\nu = 1$) excited by a blackbody source was used to monitor the rate of vibrational energy transfer. Order of magnitude calculations for the variety of V-V and V-T processes possible in these systems were used to select reasonable relaxation channels. These feasibility calculations together with decay measurements on several concentrations of CO and its collision partners enabled liquid state relaxation rate constants to be assigned. For the CO-CD₄ and CO-CF₄ systems, near-resonance energy transfer and conditions of concentration enabled us to measure the V-T rate constants for the first time for the relaxation of CD₄ and CF₄ by liquid Ar. These V-V and V-T rate constants were compared with the gas phase values obtained at the same temperature. We find that the liquid phase and gas phase rate constants are essentially the same. These results are found to be in reasonable accord with the predictions of simple models of vibrational relaxation in the liquid state.

I. INTRODUCTION

Rates of vibrational relaxation of CO ($\nu = 1$) by CH₄, CD₄, and CF₄ have been measured over a wide range of temperatures in the gas phase and possible relaxation channels have been explored.¹⁻⁶ The behavior of these systems in the liquid state has not been studied. In the gas phase even though the intermolecular potentials may be poorly understood, the dynamics of the problem of relaxation is simplified because energy is transferred by binary collisions. However in liquids, if many-body collisions are important to the relaxation process the theoretical treatment would be exceedingly difficult.

The theory of liquid state vibrational relaxation has been considered by many investigators where simplifications have been introduced. Litovitz and Madigosky^{7,8} first offered the isolated binary collision (IBC) model of liquids which assumes, as in the gas phase, that only binary collisions are responsible for vibrational energy transfer processes. Their model predicts the relaxation rate in the liquid state by scaling the gas phase rate, at the same temperature, by the increased collision frequency expected at high density. In later variations of the IBC model scaling the relaxation rate by collision frequency has been replaced by scaling by density and pair distribution function.⁹⁻¹¹ Here agreement between theory and experiment depends on the value one believes the pair distribution function should have.¹²⁻¹⁴ Both theory and experiment are however in reasonable agreement since the *rate constants* for vibrational relaxation usually agree within a factor of 2.¹⁵ A rather extensive literature provides discussion of these theoretical models and is contained in several reviews.¹⁵⁻¹⁷ We shall be testing these models for our systems.

This paper develops in the following order. Following a presentation of experimental details and results, a general discussion of relaxation kinetics is presented. A theoretical

model for selecting relaxation channels is then prepared. The systems CO-CH₄, CO-CD₄, and CO-CF₄ are then treated in turn and specific rate constants deconvoluted from the relaxation measurements. Finally these liquid state rate constants are compared with gas phase values in the light of predictions by the IBC model.

II. EXPERIMENTAL

The experimental apparatus used was similar to that described by Chandler and Ewing.¹⁸ The light emitted by a global was collected and focused into the cell to excite CO to the $\nu = 1$ level. The fluorescence from CO was collected by a spherical mirror, chopped at 13 Hz, and focused into a Perkin-Elmer model 210-B monochromator with a grating blazed at $3.75\ \mu$ and detected by a photovoltaic InSb detector cooled to 77 K. The monochromator was tuned to the peak of the emission and the slits opened to a bandpass of $35\ \text{cm}^{-1}$. Fluorescence decay followed shuttering the global exciting source. The signal from the detector was amplified and sent into a Fabri-Tek model 1074 signal averager triggered by a pulse taken from the shutter. Around 1000 decays were averaged and recorded.

Highly purified gases were used. Ar, from Matheson Gas Products, with stated purity of 99.9995% was further purified of CO₂ and H₂O by means of Linde type 4A molecular sieve cooled to dry ice temperature. CH₄ and CF₄ also from Matheson Products with stated purities of 99.0% and 99.7%, and "Research Grade" CD₄ from M-S-D Isotopic Products with minimum isotopic purity of 99 atom % deuterium were not further purified. Airco "Research Grade" CO was used with stated purity of 99.99%. It was passed through a column containing Linde type 4A molecular sieve cooled to liquid N₂ temperature for further purification.

Several concentrations with different ratios of CO-dopant were studied. Each CO-dopant mixture was prepared one day in advance of condensing the liquid to insure homogeneity. On the day of the experiment, the desired amount of

^{a)}Supported by a grant from the National Science Foundation.

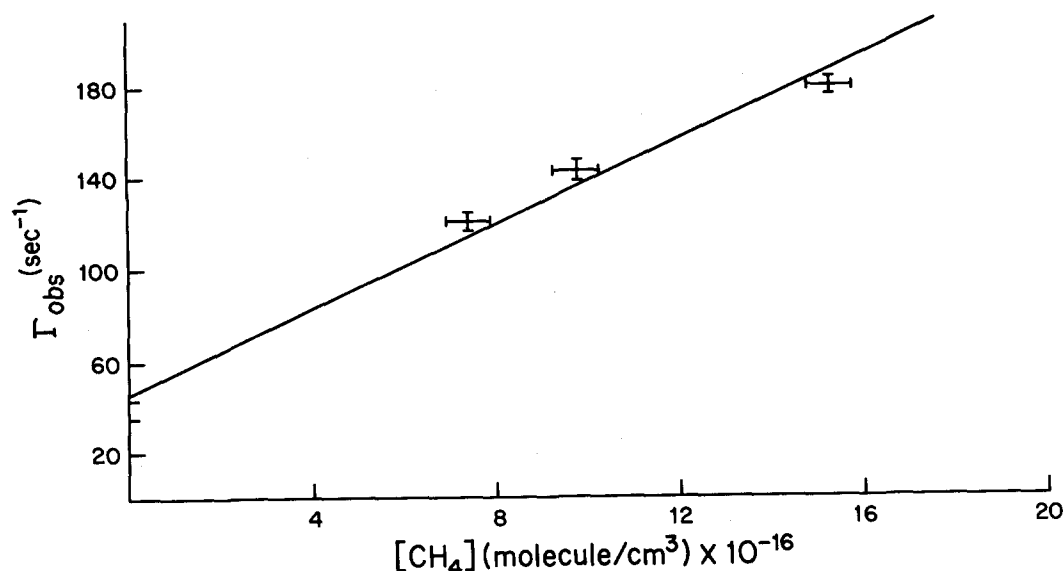


FIG. 1. Observed vibrational relaxation rates of CO by CH₄ as a function of CH₄ concentration. The CO concentration was 2.8×10^{18} molecules cm⁻³.

this mixture was introduced into the cell at room temperature. The cell was cooled to liquid Ar temperature and then the purified Ar was condensed on top of the CO-dopant mixture. The concentration of CO in liquid Ar was checked by taking the IR spectrum of the liquid solution. The temperature of the liquid was determined to be 87 ± 1 K by measurement of its vapor pressure.

III. RESULTS

All our results are presented in Figs. 1–3. The data at the intercepts give the relaxation rate of vibrationally excited

CO in argon solution in the absence of CH₄, CD₄, or CF₄. For $[\text{CO}] = 2.8 \times 10^{18}$ molecule cm⁻³, corresponding to a mole fraction of 1.3×10^{-4} we find from Fig. 1 and from the upper data points in Figs. 2 and 3 $\Gamma_{\text{obs}} = 40 \pm 4$ s⁻¹. At a higher concentration, $[\text{CO}] = 2.8 \times 10^{19}$ molecules cm⁻³, the lower data points of Figs. 2 and 3 give $\Gamma_{\text{obs}} = 23 \pm 4$ s⁻¹. These results are in agreement with Chandler's measurements¹⁸ who identified these relaxation rates with the effective radiative rate constant, $k_{\text{rad}}^{\text{eff}}$, of vibrationally excited CO. The effective radiative rate constant depends on the concentration of CO due to self-absorption and radiative

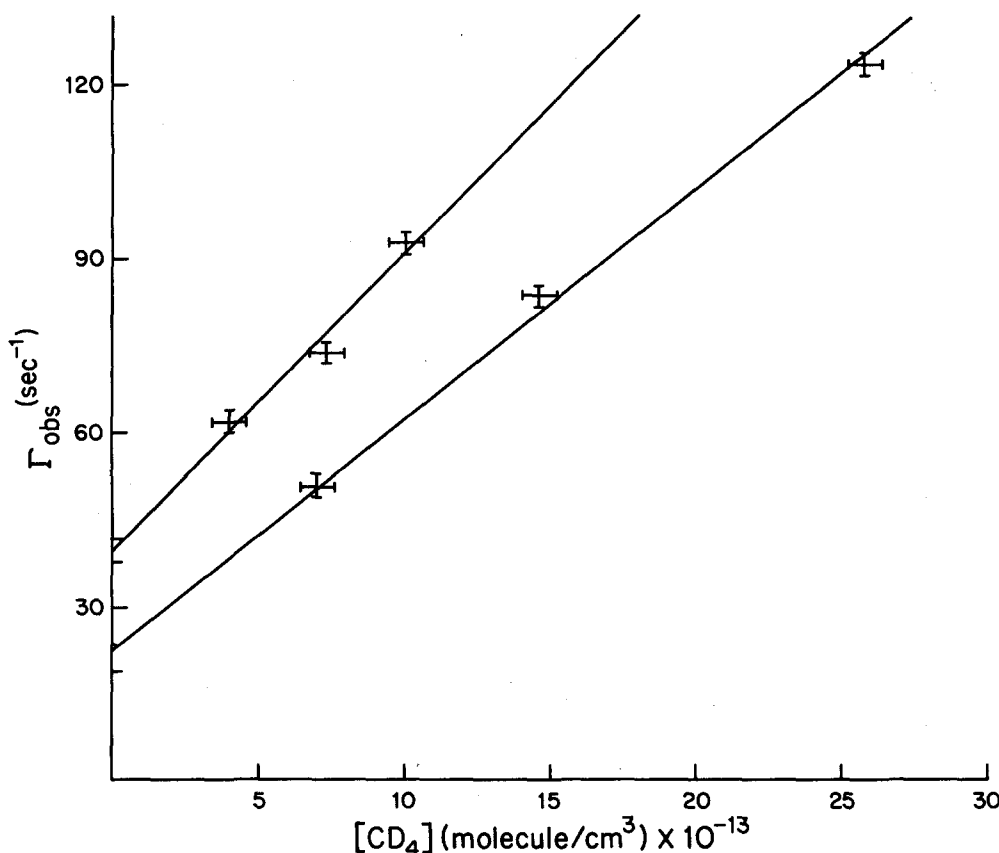


FIG. 2. Observed vibrational relaxation rates of CO by CD₄ as a function of CD₄ concentration. The upper curve is for CO concentration of 2.8×10^{18} molecules cm⁻³ and the lower curve is for CO concentration of 2.8×10^{19} molecules cm⁻³.

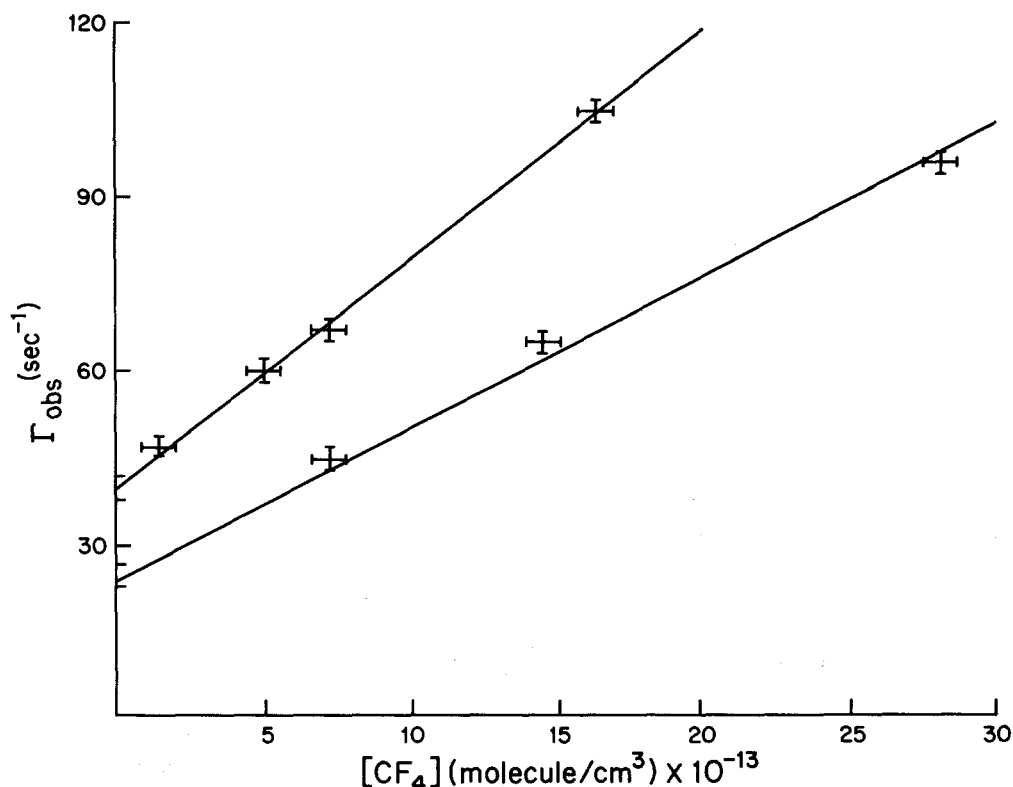


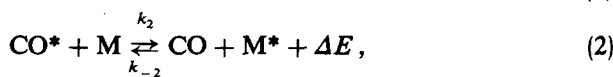
FIG. 3. Observed vibrational relaxation rates of CO by CF₄ as a function of CF₄ concentration. The upper curve is for CO concentration of 2.8×10^{18} molecules cm⁻³ and the lower curve is for CO concentration of 2.8×10^{19} molecules cm⁻³.

trapping. At higher concentrations of CO the system relaxes more slowly. Addition of CH₄, at parts per million levels or CD₄ or CF₄ at parts per billion levels increases the relaxation rate of vibrationally excited CO dramatically as Figs. 1–3 show. (The concentrations accurate to 10% may be read directly from the figures.) In all cases there is a linear relationship between Γ_{obs} and the concentrations of CH₄, CD₄, or CF₄. The data in Figs. 2 and 3 show from their slopes that CD₄ and CF₄ are more effective at lower concentrations of CO. In order to deconvolute these data to obtain specific relaxation rate constants, models for the relaxation channels are needed. These will be developed below and each system will be analyzed in turn.

IV. DISCUSSION

A. Kinetics equations

The vibrational energy levels for CO, CH₄, CD₄, and CF₄ are shown in Fig. 4. Following excitation of CO to its $\nu = 1$ vibrational state by the global source, the kinetics of the liquid mixture can be represented by the following equations:



where the asterisks indicate vibrational excitation. The effective radiative rate constant for CO*, $k_{\text{rad}}^{\text{eff}}$, depends on CO concentration because of radiative trapping.^{18,19} The V–V rate constants are k_2 and k_{-2} , for the forward and reverse

transfer of energy between CO* and the dopant M (M = CH₄, CD₄, or CF₄). The deactivation rate constant of the excited dopant by Ar is k_3 . The V–T relaxation rate of CO* by Ar is negligible compared to the radiative rate.¹⁸ Relaxation of CO* by M through the V–T channel may be ignored compared to the more efficient V–V channels of Eq.

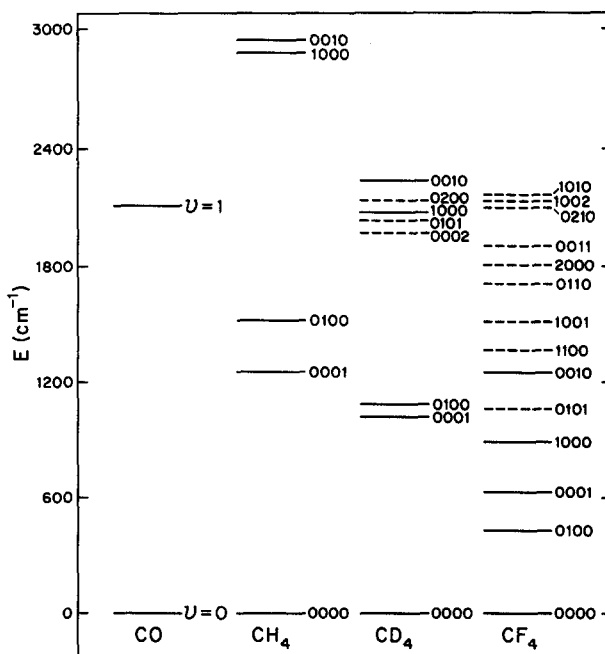


FIG. 4. Energy level diagram for CO, CH₄, CD₄, and CF₄. Solid lines represent fundamental levels and dashed lines are for overtone and combination levels. For CF₄, levels with total vibrational quanta of $\nu > 2$ were deleted for simplicity with the exceptions of (1002) and (0210).

(2). Finally, the deexcitation of M* by CO, CO*, M, and M* can be ignored due to the very low concentration of those species compared to Ar. We will, however, carefully test some of these assumptions later in the paper.

The behavior of this kinetic system can be expressed analytically by the rate equations below:

$$-\frac{d[\text{CO}^*]}{dt} = k_{\text{rad}}^{\text{eff}}[\text{CO}^*] + k_2[\text{CO}^*][\text{M}] - k_{-2}[\text{CO}][\text{M}^*], \quad (4)$$

$$-\frac{d[\text{M}^*]}{dt} = -k_2[\text{CO}^*][\text{M}] + k_{-2}[\text{CO}][\text{M}^*] + k_3[\text{M}^*][\text{Ar}], \quad (5)$$

where [X] is the concentration of species X in molecules cm⁻³. The solution for the time dependent concentration of CO* from these coupled differential equations is²⁰

$$[\text{CO}^*] = A_1 e^{-\lambda_1 t} + A_2 e^{-\lambda_2 t}, \quad (6)$$

where

$$\lambda_{1,2} = 1/2 [R_1 \pm (R_1^2 - 4R_2)^{1/2}], \quad \lambda_1 > \lambda_2, \quad (7)$$

$$R_1 = k_{\text{rad}}^{\text{eff}} + k_2[\text{M}] + k_{-2}[\text{CO}] + k_3[\text{Ar}], \quad (8)$$

$$R_2 = k_{\text{rad}}^{\text{eff}} k_{-2}[\text{CO}] + k_{\text{rad}}^{\text{eff}} k_3[\text{Ar}] + k_2 k_3[\text{M}][\text{Ar}], \quad (9)$$

and

$$\frac{A_1}{A_2} = \frac{\lambda_2 - k_2[\text{M}] - k_{\text{rad}}^{\text{eff}}}{-\lambda_1 + k_2[\text{M}] + k_{\text{rad}}^{\text{eff}}} \quad (10)$$

with

$$A_1 + A_2 = [\text{CO}^*] \text{ at } t = 0. \quad (11)$$

The relationship between the observed decay rate of CO* and the concentration of the dopant, can be evaluated using Eqs. (6)–(11). However, some simplifications of these equations can be obtained by making certain approximations which are appropriate for each dopant.

B. Locating vibrational relaxation channels

Since we have only monitored the decay from CO* it is not possible to uniquely assign a rate constant from among the variety of relaxation channels possible. As can be seen from Fig. 4 the number of levels available to accept excitation from CO* is large. Additional information is therefore needed to interpret the kinetics of these systems. In this section we shall outline a method to estimate rate constants in order to locate efficient vibrational relaxation channels.

Feasibility calculations of this sort usually follow the Schwartz, Slawsky, and Herzfeld (SSH) treatment.²¹ A single exponential function is used to mimic the repulsive portion of the intermolecular potential and a constant energy term is used to accommodate the attractive portion. However for the low temperature systems we are interested in exploring, the mean kinetic energy of the colliding molecules is comparable to the intermolecular well depth. Moreover, even the repulsive portion of the intermolecular potential function requires more than a single exponential term for realistic description.²² We prefer then the methods of Devonshire,²³ and Thompson²⁴ who obtained an analytical solution using the Morse potential to approximate the inter-

molecular potential function. Since these formulas have been previously presented in somewhat awkward form and only for V-T energy transfer, we offer them with simplified notation and include also expressions for V-V transfer not previously published.

We begin by discussing V-T relaxation of molecule A during a collision with another atom or molecule B. They collide over a Morse potential which is of the form

$$V(r) = D_e [e^{-2a(r-r_e)} - 2e^{-a(r-r_e)}], \quad (12)$$

where D_e is the well depth and r_e is the separation of A from B (measured from their respective molecular centers) at the bottom of the well. The steepness of the potential is controlled by a , the range parameter. The term which couples vibrational and translational motions from V-T relaxation is²⁵

$$V'(r, x) = V(r - S_A x) - V(r) \simeq -S_A x [dV(r)/dr]. \quad (13)$$

The effective vibrational displacement x of the molecule A is treated according to the “breathing sphere” model.²⁶ This assumes that the displacements are always normal to the surface and the degree to which they are pointing toward molecule B is contained in the steric factor S_A where $S_A^2 = 1/3$ for linear molecules and $2/3$ for nonlinear molecules. The matrix element associated with the displacement to appear in Eq. (15) is given by

$$\langle x \rangle^2 = \frac{2\bar{A}^2(v+1)\hbar^2}{W_A} \quad (14)$$

for relaxation from the $v+1$ to the v level where \bar{A}^2 is related to the normal coordinate displacements as listed elsewhere.²⁷ The vibrational energy lost by molecule A during its relaxation is W_A .

The resulting probability of V-T relaxation as a function of initial relative velocity v_m is given by²⁴

$$P(v_m) = \pi^2 S_A^2 a^2 / \langle x \rangle^2 (q_m^2 - q_n^2) \exp[\pi(q_m - q_n)] \times \left[\frac{\prod_{s=1}^d [(s-1/2)^2 + q_m^2]}{\prod_{s=1}^d [(s-1/2)^2 + q_n^2]} \right]. \quad (15)$$

The system A* + B approaches with initial de Broglie wavelength $\lambda_m = h/p = h/(2\mu_v E_m)^{1/2}$, where $\mu_v = (m_A m_B)/(m_A + m_B)$ is the reduced mass of the colliding pair. The initial energy being $E_m = 1/2(\mu_v v_m^2)$. The quantity

$$q_m = (2\mu_v E_m)^{1/2} / a\hbar \quad (16)$$

which appears in Eq. (15) is then the reciprocal of the de Broglie wavelength scaled by the range parameter. In effect q_m counts the nodes of the plane wave in the vicinity of the range, a^{-1} , of the repulsive wall of the intermolecular potential well. The comparable quantity for A + B after relaxation is

$$q_n = [2\mu_v (E_m + \Delta E)]^{1/2} / a\hbar, \quad (17)$$

where $\Delta E = W_A$, the translational energy taken up by the colliding pair in the V-T process. The well depth appears in Eq. (15) as the dimensionless parameter

$$d = (2\mu_v D_e)^{1/2} / a\hbar \quad (18)$$

which has been rounded off (by slight adjustment of a or D_e) to an integer. Since D_e and a are only approximately known, this condition does not limit our treatment. The d parameter gives the number of bound states of the Morse potential well. Another approximation that has been introduced in deriving Eq. (15) is that $\pi q_{m,n} \gg 1$, a condition easily met in V-T transfer for our system.

The Thompson model has been extended to the V-V channel.²⁸ The coupling term for the V-V process is given by²⁵

$$V'(r, x, y) \simeq S_A S_B xy [d^2 V(r) / dr^2], \quad (19)$$

where y and S_B are the corresponding displacement and steric factors for the molecule B. The result for the probability²⁸ is

$$P(v_m) = 4\pi^2 a^4 S_A^2 S_B^2 \langle x \rangle^2 \langle y \rangle^2 \frac{\sinh 2\pi q_m \sinh 2\pi q_n}{(\cosh 2\pi q_m - \cosh 2\pi q_n)^2} \times \frac{[(q_n^2 - q_m^2 + d)A_n + (q_n^2 - q_m^2 - d)A_m]^2}{A_n A_m} \quad (20)$$

$$\text{with } A = \cosh \pi q \prod_{s=1}^d [(s - 1/2)^2 + q^2] \quad (21)$$

and $\langle y \rangle^2$ given by a term analogous to Eq. (14) containing W_B as the vibrational energy accepted by molecule B. The translational energy taken up by the colliding pair in the V-V process is $\Delta E = W_A - W_B$ which must be inserted into Eq. (17).

The transition probability $P(v_m)$ is dependent on the initial velocity v_m . We must therefore average over all initial velocities at temperature T to find the average transition probability. The result is

$$\langle P(T) \rangle = \left(\frac{\mu_v}{2kT} \right)^2 \int_0^\infty v_m^3 P(v_m) \exp(-\mu_v v_m^2 / 2kT) dv_m. \quad (22)$$

This integral must be evaluated numerically.

The V-T and V-V rate constants are calculated from the corresponding probability by²⁹

$$k(T) = \langle P(T) \rangle (8\pi kT / \mu_v)^{1/2} \sigma_{A,B}^2. \quad (23)$$

Here $\sigma_{A,B} = 1/2(\sigma_A + \sigma_B)$, where σ_A and σ_B are the hard sphere diameters for molecules A and B, respectively. The rate constant $k(T)$ is given in units of molecule⁻¹ cm³ s⁻¹.

Description of intermolecular interactions for the molecules we shall consider are usually provided by the Lennard-Jones (6-12) potential.³⁰ We are left then with the task of fitting the Morse potential to the (6-12) potential. Using methods outlined elsewhere³¹ we find $a = 2 \times 10^8$ cm⁻¹ for the range parameter which is in reasonable agreement with the comparable repulsive parameter usually used in the SSH treatment.²⁵ We shall use this range parameter throughout the paper in our calculations.

Evaluating the transition probability for V-T channels in which the total change in vibrational quantum number is $\Delta v > 1$ and for V-V channels where $\Delta v > 2$ would require coupling terms of higher order than those in Eqs. (13) or (19). In addition, the wave functions describing vibrations of molecules A or B would need to be those of anharmonic oscilla-

tors. To sidestep all these complications and in keeping with our modest goal to obtain only order of magnitude results we fall back on an empirical estimate of Rapp.³² For V-T channels the probability calculated by Eq. (15) is multiplied by a factor of $(10^{-2})^{\Delta v - 1}$ for $\Delta v > 1$ and for V-V channels Eq. (20) is multiplied by $(10^{-2})^{\Delta v - 2}$ for $\Delta v > 2$.

One drawback of the SSH or Thompson models is that they do not consider the dipole-dipole interaction which plays an important role in near resonant transitions involving infrared active modes. Mahan³³ has investigated the magnitude of this long-range dipole-dipole interaction for near resonant vibrational energy exchange processes and found probabilities for V-V energy transfer orders of magnitude greater than those estimated using only an exponential repulsive interaction potential between molecules. Stephenson *et al.*³⁴ found however, that energy-transfer probabilities for the long-range interaction decrease rapidly with increasing energy gap, ΔE , for a transition. When $\Delta E > 250$ cm⁻¹ the shorter range interactions are observed to give larger energy transfer probabilities than the dipole-dipole interactions. A more detailed discussion on the effect of energy gap and temperature on V-V transfer probabilities caused by long-range interactions is given by Yardley.³⁵ In summary, both the dipole-dipole interaction and the energy gap in the transition have to be considered for a realistic prediction of energy transfer probabilities.

Another possible drawback in the feasibility treatment we have just presented is the neglect of rotational motions in the vibrational relaxation process. The rotational contribution to yield V-T,R channels has been considered by Nikitin³⁶ and to the methanes by Zittel and Moore.³⁷ Their results suggested that the rotational velocity of the collision partner can play a role in the relaxation process, effectively increasing the collision velocity and thus increasing the energy transfer probability. In our work, the energy gaps in the relaxation processes are often very small, which makes V-V relaxation take place on a very short time scale. Also, since we are interested in relative rather than absolute values of the probabilities for the various transitions, we have neglected these rotational contributions.

C. CO-CH₄

The vibrational level of the CH₄ molecule which accepts the excitation from CO* in Eq. (2) is not known experimentally. Millikan¹ considered the most likely transfer to be to the (0100) level at 1534 cm⁻¹ because it has the minimum energy gap ($\Delta E = 609$ cm⁻¹) below the donor level. Green and Hancock² who measured the relaxation rate of CO* by CH₄ at 298 K, considered (0001) at 1306 cm⁻¹ the acceptor level ($\Delta E = 834$ cm⁻¹) because of its large infrared transition dipole moment to the ground state. Gregory *et al.*⁶ likewise favored transfer to the (0001) level. However, as we have already argued, it is the short range interactions rather than the long range transition dipole terms which determine the energy transfer rates when $\Delta E > 250$ cm⁻¹. Using the Morse calculation based on Thompson's model, the rate constants for the V-V transition to the (0100) and (0001) levels are 1×10^{-15} and 6×10^{-17} molecule cm³ s⁻¹, respectively, at

87 K. Here we have taken³⁰ $D_e = 2 \times 10^{-14}$ erg for CO + CH₄ together with $a = 2 \times 10^8$ cm⁻¹ to obtain $d = 4$, $\langle x \rangle^2 = 1.7 \times 10^{-18}$ cm² and $\langle y \rangle^2 = 2.3 \times 10^{-17}$ cm² from values of \bar{A}^2 given elsewhere,^{26,27} $S_A^2 = 1/3$, $S_B^2 = 2/3$, and³⁰ $\sigma_{A,B} = 3.8 \times 10^{-8}$ cm. With this, k_2 is dominated by the V-V rate between CO* and CH₄(0100) in agreement with Millikan's¹ preference and previous SSH calculations.³⁸

The backward rate constant k_{-2} for the V-V process between CH₄* and CO is much smaller than k_2 for the forward process. From microscopic reversibility, $k_{-2} = k_2 \exp(-\Delta E/kT)$, for $\Delta E = 609$ cm⁻¹ and $kT = 60$ cm⁻¹ at 87 K, $k_{-2} = 4 \times 10^{-5} k_2$ so k_{-2} may be ignored. With this, Eq. (4) becomes

$$-\frac{d[\text{CO}^*]}{dt} = (k_2[\text{CH}_4] + k_{\text{rad}}^{\text{eff}})[\text{CO}^*]. \quad (24)$$

The observed first order decay of the CO* fluorescence provides the rate

$$\Gamma_{\text{obs}} = k_2[\text{CH}_4] + k_{\text{rad}}^{\text{eff}}. \quad (25)$$

A plot of Γ_{obs} vs $[\text{CH}_4]$ is shown in Fig. 1, its slope yields $k_2 = (9.3 \pm 0.9) \times 10^{-16}$ molecule⁻¹ cm³ s⁻¹ and the intercept $k_{\text{rad}}^{\text{eff}} = 40$ s⁻¹ in agreement with Chandler¹⁸ for $[\text{CO}] = 2.8 \times 10^{18}$ cm⁻³. With the necessary approximations made in our estimate of the rate constant we view the calculated value $k_2 = 1 \times 10^{-15}$ molecule⁻¹ cm³ s⁻¹ to be in fortuitous agreement with the measured value.

Richman and Millikan³ measured the rate constant for the V-V energy exchange between CO* and CH₄ in the gas phase between 400–100 K. Extrapolating their data to 87 K yields a value of 1.2×10^{-15} molecule⁻¹ cm³ s⁻¹. Allen *et al.*⁵ measured the gas phase relaxation rate for CO-CH₄ at 87 K and obtained a value of 1.2×10^{-15} molecule⁻¹ cm³ s⁻¹. Full discussion and comparison between the gas phase and the liquid phase rate constants will be given in a separate section as a test for the IBC model.

Calaway and Ewing³⁹ measured the V-V rate constant for the relaxation of N₂* by CH₄ to be $(8.1 \pm 1.7) \times 10^{-17}$ molecule⁻¹ cm³ s⁻¹, which is an order of magnitude smaller than ours. However, the larger energy gap between N₂* and CH₄(0100) ($\Delta E = 800$ cm⁻¹) is expected to make the V-V transfer slower. For the sake of comparison with the CO*/CH₄(0100) system, the Morse V-V calculations for N₂*/CH₄(0100) were performed at 77 K. Using $\langle x \rangle^2 = 1.2 \times 10^{-18}$ cm² and all other parameters with their previous values we find $k_2 = 7 \times 10^{-17}$ molecule⁻¹ cm³ s⁻¹. The ratio of the calculated rate constants: $k_2^{\text{CO}^*-\text{CH}_4}/k_2^{\text{N}_2^*-\text{CH}_4} = 14$ is in reasonable agreement with the ratio of the measured rate constants of $k_2^{\text{CO}^*-\text{CH}_4}/k_2^{\text{N}_2^*-\text{CH}_4} = 11$. This agreement is further support for the assignment of (0100) of CH₄ as the acceptor level.

D. CO-CD₄

The vibrational mode of CD₄ which is initially excited by CO* has not been determined experimentally. Among all levels of CD₄ close to the $\nu = 1$ level of CO (see Fig. 4), transitions to the fundamental levels (1000) or (0010) are expected to be the most likely. Our calculations which bear out these expectations use all the parameters listed for CO*-

CH₄ except $\langle y \rangle^2 = 6 \times 10^{-19}$ cm² an approximate value we use for all the possible CD₄ accepting modes.²⁷ In addition, we have estimated transitions from CO($\nu = 1$) to the (0200), (0101), and (0002) levels near 2100 cm⁻¹ which we find are one or two orders of magnitude less efficient since each transfer involves a total quanta change of 3. From the results shown in Table I it is clear that the (1000) level with $k_2 = 4 \times 10^{-13}$ molecule⁻¹ cm³ s⁻¹ is the major recipient of vibrational energy from CO*. Another argument favoring transition to (1000) is the inverse temperature dependence of the relaxation rate constant⁵ which is characteristic of near resonance energy transfer processes.³⁵

The vibrational energy of CD₄(1000) can either go back to CO, or it can be redistributed, by V-V processes, among the four other fundamental and combination levels of CD₄ around 2100 cm⁻¹. We propose that a pseudoequilibrium can be established among these levels. There are two reasons which lead us to believe that such pseudoequilibrium exists. First, the energy gaps among these levels are small and consequently the rate of redistribution of vibrational energy is much faster than the rate of transitions to low-lying CD₄ levels around 1000 cm⁻¹. Second, due to the large concentration of Ar compared to CO, CD₄(1000) has a greater chance of colliding with Ar and redistributing its energy with the adjacent levels rather than colliding with diluted CO and giving it back the vibrational energy.

In order to explore the fate of CD₄(1000) we have performed additional calculations. In the middle section of Table I labeled k_s we estimate the rate constants which move CD₄* in (1000) to the nearby levels (0010), (0200), (0101), and (0002). As shown these scrambling rate constants are $k_s \sim 10^{-13}$ molecule⁻¹ cm³ s⁻¹. Since CD₄* is in a bath dominated by collisions with $[\text{Ar}] \sim 10^{22}$ molecules cm⁻³ the scrambling occurs at a rate of $\sim 10^9$ s⁻¹. This rate is three orders of magnitude faster than the efficient CD₄(1000) + CO($\nu = 0$) process since $k_{-2} \simeq k_2 \simeq 10^{-13}$ molecule⁻¹ cm³ s⁻¹ and $[\text{CO}] \sim 10^{19}$ molecules cm⁻³ giving a rate of $\sim 10^6$ s⁻¹. It is also many orders of magnitude faster than the relaxation of CD₄(1000) to the low-lying levels CD₄(0100) and CD₄(0001) near 1000 cm⁻¹. Here our feasibility calculations for this process, shown in the lower section of Table I, gives a rate constant $k_3 \sim 10^{-18}$ molecule⁻¹ cm³ s⁻¹. Using $[\text{Ar}] \sim 10^{22}$ molecules cm⁻³ we obtain a rate of $\sim 10^4$ s⁻¹. A pseudoequilibrium is therefore established among the levels (1000), (0200), (0101), and (0002) in a time of $\tau \sim 10^{-9}$ s. A Boltzmann distribution among these levels near 2100 cm⁻¹ can therefore be calculated and is presented in Table II. This table shows the levels participating in the pseudoequilibrium, their degeneracy, energy spacing relative to (0002) the lowest level in the group, and the normalized populations.

Using the concept of pseudoequilibrium, the kinetics of CO-CD₄ can be written as follows:

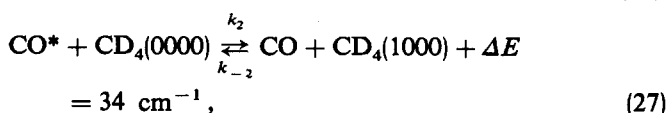
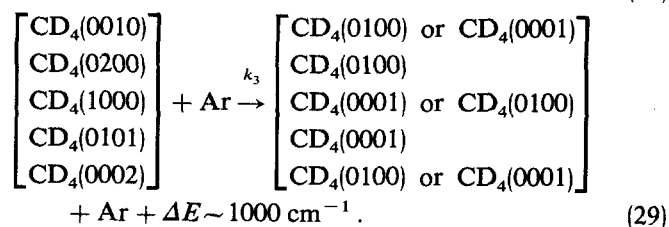
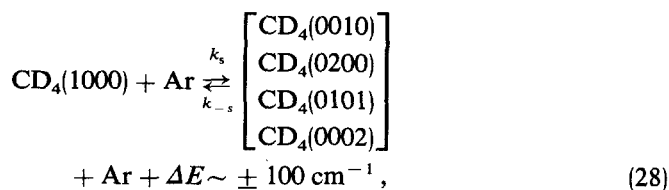


TABLE I. Theoretical vibrational relaxation rate constants: CO-CD₄ in liquid argon.

Type of rate constant	Transition	ΔE (cm ⁻¹)	Vibrational quanta change	k (molecule ⁻¹ cm ³ s ⁻¹)
k_2	CO* → CD ₄ (0010)	-116	2	3.0×10^{-14}
	CD ₄ (0200)	-41	3	2.1×10^{-15}
	CD ₄ (1000)	34	2	4.4×10^{-13}
	CD ₄ (0101)	55	3	4.1×10^{-15}
	CD ₄ (0002)	151	3	1.5×10^{-15}
k_s	1000 → 0010	-150	2	5.7×10^{-13}
	0200	-75	3	9.4×10^{-14}
	0101	21	3	9.0×10^{-13}
	0002	117	3	1.4×10^{-13}
k_3	1000 → 0100	1017	2	1.1×10^{-18}
	0001	1113	2	2.7×10^{-19}
	0010 → 0100	1167	2	1.2×10^{-19}
	0001	1263	2	3.1×10^{-20}
	0200 → 0100	1092	1	3.7×10^{-17}
	0001	1188	3	9.0×10^{-22}
	0101 → 0100	996	1	1.6×10^{-16}
	0001	1092	1	3.7×10^{-17}
	0002 → 0100	900	3	6.9×10^{-20}
	0001	996	1	1.6×10^{-16}



In applying the rate equations (4) and (5) to the CO-CD₄ system, [M*] in the expression $k_{-2}[\text{CO}][\text{M}^*]$ must be replaced by $1.3 \times 10^{-2}[\text{CD}_4(1000)]$, where the factor 1.3×10^{-2} from Table II is the concentration of CD₄(1000) relative to other CD₄* in the pseudoequilibrium group. [M*] in the expression $k_3[\text{M}^*][\text{Ar}]$ of Eq. (5) remains unchanged because [M*] is now representing CD₄(0101) and CD₄(0002) which have essentially unit relative concentrations (see Table II).

TABLE II. Pseudoequilibrium populations of CD₄ levels.

Levels	g_i^a	ΔE_i (cm ⁻¹) ^b	N_i^c
0010	3	267	2.8×10^{-3}
0200	4	192	1.5×10^{-2}
1000	1	117	1.3×10^{-2}
0101	6	96	1.1×10^{-1}
0002	9	0	8.5×10^{-1}

^a g_i = degeneracy.

^b ΔE_i = energy gap between level i and the lowest energy level: (0002).

^c $N_i = (g_i e^{-\Delta E_i/kT}) / \sum_j g_j e^{-\Delta E_j/kT}$, the normalized population of level i .

Knowing that the radiative rate is much slower than the V-V rates, and examining the relative concentration of the species involved, $[\text{CD}_4]:[\text{CO}]:[\text{Ar}] \approx 10^{-8}:10^{-4}:1$, one can ignore the k_{rad} and $k_2[\text{CD}_4]$ terms in Eq. (8), and R_1 can be written as

$$R_1 \sim 1.3 \times 10^{-2} k_{-2}[\text{CO}] + k_3[\text{Ar}]. \quad (30)$$

With all the terms in R_2 of Eq. (9) retained, and since $R_1^2 \gg R_2$ ($R_1 \sim 10^5$ and $R_2 \sim 10^7$) one can expand Eq. (7) to

$$\lambda_{1,2} \sim 1/2 [R_1 \pm R_1(1 - 2R_2/R_1^2)]. \quad (31)$$

This yields

$$\lambda_1 \sim R_1,$$

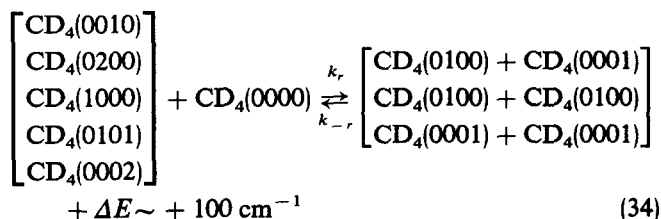
$$\lambda_2 \sim R_2/R_1. \quad (32)$$

λ_1 is too fast to be measured with our apparatus, so the observed rate corresponds to λ_2 .

Using Eq. (9), (30), and (32), and considering the effect of the pseudoequilibrium on k_{-2} , one can write

$$\Gamma_{\text{obs}} = \lambda_2 \sim k_{\text{rad}}^{\text{eff}} + \left[\frac{k_2 k_3 [\text{Ar}]}{1.3 \times 10^{-2} k_{-2} [\text{CO}] + k_3 [\text{Ar}]} \right] [\text{CD}_4]. \quad (33)$$

In the treatment above we have ignored, without justification, the self relaxation of CD₄. Consider the efficient near-resonant relaxation processes,



which would serve to upset the scrambling reactions of Eq. (28) and the relaxation processes of Eq. (29). It is the low concentration of CD₄(0000) which renders the relaxations of Eq. (34) ineffective despite the large k_r rate constants. We use our feasibility calculations for the efficient relaxation: CD₄(0002) + CD₄(0000) → 2CD₄(0001) + ΔE = −5 cm^{−1}. Taking Eqs. (20)–(23) with $S_A^2 = S_B^2 = 2/3$, $a = 2 \times 10^8$, $\langle x \rangle^2 = \langle y \rangle^2 = 6 \times 10^{-19}$ cm², $d = 4$ and $\sigma_{A,B} = 3.8 \times 10^{-8}$ cm we find $k_r = 5 \times 10^{-11}$ cm³ molecule^{−1} s^{−1}. [This value is within an order of magnitude of the experimentally measured rate $k = 0.7 \times 10^{-11}$ cm³ molecule^{−1} s^{−1} of a similar process⁴⁰ in which CH₄(0010) relaxes on collision with CH₄(0000).] For typical CD₄ concentrations of $\sim 10^{14}$ molecules cm^{−3} we have $k_r[\text{CD}_4] \sim 5 \times 10^3$ s^{−1} which is slower by six orders of magnitude than our previous estimate of $k_s[\text{Ar}]$. We see then that the scrambling processes of Eq. (28) occur without competition from self-relaxation and psuedoequilibrium is established. Relaxation from the lowest levels of the psuedoequilibrium manifold is calculated (see Table I) to be $k_3 \sim 10^{-16}$ cm³ molecule^{−1} s^{−1} so $k_3[\text{Ar}] \sim 10^6$ s^{−1} which is several orders of magnitude faster than the self-relaxation rate. We conclude then that self-relaxation does not compete with relaxation by Ar in the processes of Eq. (29). Were self-relaxation to be important (e.g. at high concentrations of CD₄), an additional term, $k_2 k_r[\text{CD}_4]$, would need to be introduced into the numerator and denominator of the expression in brackets in Eq. (33). A nonlinear relationship between Γ_{obs} and $[\text{CD}_4]$ would then result. As can be seen in Fig. 2 a clear linear relationship between Γ_{obs} and $[\text{CD}_4]$ is found.

From the two slopes in Fig. 2 and Eq. (33) using $k_{-2} = 0.6k_2$ consistent with Eq. (27) and $T = 87$ K we obtain $k_2 = (5.1 \pm 0.8) \times 10^{-13}$ molecule^{−1} cm³ s^{−1} and $k_3 = (1 \pm 0.4) \times 10^{-17}$ molecule^{−1} cm³ s^{−1}. These two collisional vibrational relaxation rate constants are in reasonable agreement with our feasibility calculations of Table I as we associate k_2 with Eq. (27) and k_3 with either CD₄(0002) + Ar → CD₄(0001) + Ar and/or CD₄(0101) + Ar → CD₄(0100) + Ar. These rate constants are also consistent with the concept of psuedoequilibrium as we have shown.

Allen *et al.*⁵ have measured the gas phase V–V rate constant for CO*–CD₄ in Ar. The system was studied in the temperature range between 293 and 80 K, but with much higher relative concentration of CD₄ than we used. Under their experimental conditions, the excited CD₄ molecules relax to lower vibrational states faster than the initial V–V process. This they showed by the addition of H₂, which will remove ~ 1000 cm^{−1} of energy rapidly from CD₄* while having little effect on CO*. They found that the rate for the vibrational deactivation of CO* by CD₄ is almost the same with and without the addition of H₂ to the system. At 87 K, the value of their V–V rate constant, which we interpret to be k_2 , is 5.1×10^{-13} molecule^{−1} cm³ s^{−1} in agreement with our liquid state value.

The rate constant for the vibrational deactivation of CD₄(0001) and CD₄(0100) to the ground state by Ar, has been measured by Gregory *et al.*⁴¹ in the gas phase between 294 and 105 K using a laser fluorescence technique. Extra-

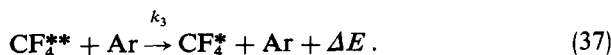
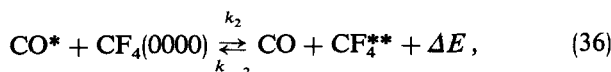
polarization of their results to 87 K, yields a value of 1.1×10^{-17} molecule^{−1} cm³ s^{−1} consistent with our $k_3 = (1 \pm 0.4) \times 10^{-17}$ molecule^{−1} cm³ s^{−1}. This agreement is expected since they measured the rate for processes similar to those we are considering: CD₄(0002) + Ar → CD₄(0001) + Ar and/or CD₄(0101) + Ar → CD₄(0100) + Ar in terms of the collision partner (Ar), energy gap (ΔE ~ 1000 cm^{−1}) and number of vibrational quanta changed (Δν = 1).

Manzanares and Ewing⁴² measured the relaxation rate for CD₄(0010) by N₂ following V–V energy transfer from N₂* to CD₄(0000). Since their concentrations of N₂ were 10⁴ times as great as our concentrations of CO no psuedoequilibrium could be established in their system. Their rate constant, $k = 2 \times 10^{-16}$ molecule^{−1} cm³ s^{−1}, is then presumably some complex combination of what we have called k_2 and k_3 .

E. CO–CF₄

One might expect the V–V relaxation of CO* by CF₄ to be slower than that of CO* by CH₄. While both systems have similar symmetry, CF₄ has a greater energy mismatch between its closest fundamental level and CO*, it has a greater mass, and a larger moment of inertia, which excludes the possibility of V–R channels that may augment the observed V–V rate to CF₄. However, we found in the liquid as in the gas phase,^{2,3,5} that the V–V rates in the CO–CF₄ system to be more than two orders of magnitude faster than that for CO–CH₄. This rules out the possibility that the transfer goes to the closest fundamental level [(0010) at 1281 cm^{−1}] of CF₄. Richman and Millikan³ found an inverse temperature dependence of the rate constant for CO–CF₄, which is usually an indication of near resonance energy transfer, and suggested levels (1010), (1002) and (0210) to be the recipients of vibrational energy from CO*. Our V–V calculations were performed for the transitions between CO* and the various overtones and combinational levels of CF₄. The calculations suggest that the level (1010) is the major recipient of vibrational energy from CO*. These calculations, using the rules outlined in Sec. IV B, indicate that the transition to (1010) to be five orders of magnitude more likely than to (0010) the nearest fundamental level. Transitions to other nearby levels (1002) and (0210) which involve total changes in vibrational quantum numbers of 3 or 4 may also have significant rate constants. Indeed the infrared spectra of CF₄ in liquid argon⁴³ shows comparable oscillator strength to the levels (1010), (1002), and (0210) suggesting that the normal modes and the corresponding quantum numbers are poorly defined. Somewhat arbitrarily then we take k_2 to measure the transfer from CO* producing the cluster of CF₄ states (1010), (1002), and (0210) which we call CF₄*. Our calculations suggest that the scrambling rate constant k_s among these states is comparable to relaxation k_3 to nearby lower combination levels such as (0011), (2000), etc. which we call CF₄*. We do not therefore anticipate a psuedoequilibrium to be established as in the case of CD₄. Once the system lands at (0011) or below, the irreversible cascade down the vibrational ladder proceeds.

The kinetics of CO–CF₄ system can therefore be written as follows:



Following the same method to solve the rate equations as before, the observed rate of the CO–CF₄–Ar system becomes

$$\Gamma_{\text{obs}} = \lambda_2 = k_{\text{rad}}^{\text{eff}} + \left[\frac{k_2 k_3 [\text{Ar}]}{k_{-2} [\text{CO}] + k_3 [\text{Ar}]} \right] [\text{CF}_4]. \quad (38)$$

Because the V–V transitions described by Eq. (36) involve a number of levels the rate $k_{-2} = k_2 \exp(-\Delta E/kT)$ is not precisely defined. However, the levels for CO($v=1$) and CF₄ states (1010), (1002), and (0210) are essentially isoenergetic so we take $k_2 \simeq k_{-2}$. From the two slopes in Fig. 3 corresponding to different CO concentrations and Eq. (38) we find $k_2 = (4 \pm 0.8) \times 10^{-13} \text{ molecule}^{-1} \text{ cm}^3 \text{ s}^{-1}$ and $k_3 = (1.0 \pm 0.5) \times 10^{-14} \text{ molecule}^{-1} \text{ cm}^3 \text{ s}^{-1}$.

Richman and Millikan³ measured the temperature dependence of CO* collisional transfer rate by CF₄ between 350 and 100 K. Extrapolating their data to 87 K gives a value of $2.6 \times 10^{-13} \text{ molecule}^{-1} \text{ cm}^3 \text{ s}^{-1}$ for the V–V transfer rate constant, which corresponds to our k_2 . A similar extrapolation of the results of Allen *et al.*⁵ gives $k_2 = 1.6 \times 10^{-13} \text{ molecule}^{-1} \text{ cm}^3 \text{ s}^{-1}$. We know of no gas phase measurements of k_3 .

F. The IBC model

The IBC model in its earliest formulation^{7,8} gives the vibrational relaxation rate in terms of the average probability $\langle P(T) \rangle$ and the collision frequency Z of hard spheres such that

$$\tau^{-1} = \langle P(T) \rangle Z. \quad (39)$$

According to the IBC model the average probability does not depend on phase so $\langle P(T) \rangle^l = \langle P(T) \rangle^g$ and Eq. (39) for the ratio of liquid phase and gas phase rate constants becomes

$$k^l/k^g = Z^l/Z^g \cdot \rho^g/\rho^l, \quad (40)$$

where we have replaced the relaxation rate τ^{-1} by the relaxation rate constant $k = \tau^{-1}\rho$ where ρ is the fluid density. Recipes for determining the collision frequency can be rather ambiguous. Davis and Oppenheim⁹ in their investigations of fluid phase collision frequencies reduced the ambiguity by considering collisions that are effective in the relaxation process rather than hard sphere collisions. The ratio of the rate constants in the liquid to that in the gas is considered to be equal to the ratio of the probabilities of finding the colliding species at the effective distance, r_{ef} , in the two phases. This is given by the ratio of the temperature and density dependent pair distribution functions. Equation (40) then becomes

$$\frac{k^l}{k^g} = \frac{g^l(r_{\text{ef}}, T, \rho)}{g^g(r_{\text{ef}}, T, 0)}. \quad (41)$$

A test of the IBC model then can be made by comparing experimental measurements of k^l/k^g with theoretical evaluations of g^l/g^g .

We shall restrict the test to the data of k_2 for CO*...CH₄ and CO*...CD₄. These data give $(k_2^l/k_2^g)^{\text{CO}^*\text{---CH}_4} = 0.8 \pm 0.1$ and $(k_2^l/k_2^g)^{\text{CO}^*\text{---CD}_4} = 1.0 \pm 0.2$ which says in effect that the rate constants are nearly the same in the gas and liquid phases. We select this system since the molecular diameters and well depths are similar³⁰ ($\sigma_{\text{Ar}} = 3.4 \text{ \AA}$, $\sigma_{\text{CO}} = 3.8 \text{ \AA}$, $\sigma_{\text{CH}_4} = \sigma_{\text{CD}_4} = 3.8 \text{ \AA}$, and $\text{De}_{\text{Ar}} = 120 \text{ K}$, $\text{De}_{\text{CO}} = 100 \text{ K}$, $\text{De}_{\text{CH}_4} = \text{De}_{\text{CD}_4} = 148 \text{ K}$) consequently the pair distribution for the solution will be approximately that for neat Ar whose fluid properties have been studied.⁴³

The first step in evaluating the pair distribution functions is an estimate of r_{ef} . This comes from first searching the integrand of Eq. (22) for the most effective velocity $v_{m,\text{eff}}$. For CO*–CH₄ with an energy gap of $\Delta E = 609 \text{ cm}^{-1}$ this becomes $v_{m,\text{eff}} = 7.0 \times 10^4 \text{ cm s}^{-1}$ and for CO*–CD₄ with $\Delta E = 34 \text{ cm}^{-1}$ we have $v_{m,\text{eff}} = 4.8 \times 10^4 \text{ cm s}^{-1}$. This may be compared with the most probable velocity from the distribution [see Eq. (22)] of $N(v) \sim v_m^3 \exp(-\mu_v v_m^2/2kT)$ which gives $v_{m,\text{MP}} = 4.6 \times 10^4 \text{ cm s}^{-1}$. Thus most collisions are energetic enough to relax CO*–CD₄ but those on the high energy tail of the Boltzmann distribution are required to relax CO*–CH₄. Rather than use the three parameter Morse potential equation (12) to evaluate r_{ef} we turn to the Lennard-Jones 6-12 potential: $V_{\text{LJ}}(r) = 4\text{De}[(\sigma/r)^{12} - (\sigma/r)^6]$ to find the position on this curve corresponding to the energy associated with $v_{m,\text{eff}}$. We find $r_{\text{ef}} = 0.97\sigma$ for CO*–CD₄ and $r_{\text{ef}} = 0.94\sigma$ for CO*–CH₄. We turn next to the problem of evaluating g now that r_{ef} , T , and ρ are known.

For the gas phase, the low density limit ($\rho \rightarrow 0$) of the pair distribution function can be expressed simply as³⁰

$$g^g(r_{\text{ef}}, T, 0) = \exp[-V_{\text{LJ}}(r_{\text{ef}})/kT]. \quad (42)$$

For values of $r_{\text{ef}} \approx \sigma$ Verlet's molecular dynamics calculations of Lennard-Jones fluids are appropriate⁴⁴ to evaluate $g^l(r_{\text{ef}}, T, \rho)$. Use of his tables for $\rho^* = \rho\sigma^3 = 0.85$ and $T^* = kT/\epsilon = 0.72$ (which is close to liquid argon at 87 K $\rho^* = 0.82$, $T^* = 0.72$) on interpolation yields $g^l/g^g = 1.7$ for $r_{\text{ef}} = 0.97\sigma$. This value appears too high for $(k_2^l/k_2^g)^{\text{CO}^*\text{---CD}_4} = 1.0 \pm 0.1$. Extrapolation of Verlet's tables or use of Chesnoy's procedure^{15,45} which adapts Anderson, Weeks, and Chandler liquid state perturbation theory⁴⁶ gives $g^l/g^g \sim 1.9$ for $r_{\text{ef}} = 0.94\sigma$. The IBC model thus predicts an increase in k^l/k^g where in fact a decrease $(k_2^l/k_2^g)^{\text{CO}^*\text{---CH}_4} = 0.8 \pm 0.1$ is observed. However, within the uncertainty of the experimental measurements of k^l/k^g and the web of assumptions required in using neat argon pair distribution function calculations for the tertiary system Ar:CO:CH₄ (or CD₄) the factor of 2 discrepancy in the theoretical and experimental rate constant values may well be reasonable.

V. CONCLUSIONS

The vibrational relaxation rate constants for energy transfer between CO and CH₄, CD₄, or CF₄ is essentially the same for gas phase and in solution with liquid argon. These

results are in reasonable accord with the predictions of the IBC model.

- ¹R. C. Millikan, *J. Chem. Phys.* **43**, 1439 (1965).
²W. H. Green and J. K. Hancock, *J. Chem. Phys.* **59**, 4326 (1973).
³D. C. Richman and R. C. Millikan, *J. Chem. Phys.* **63**, 2242 (1975).
⁴J. C. Stephenson and E. R. Mosburg, *J. Chem. Phys.* **60**, 3562 (1974).
⁵D. C. Allen and C. J. S. M. Simpson, *Chem. Phys.* **76**, 231 (1983).
⁶E. A. Gregory, M. M. Maricq, R. M. Siddles, C. T. Wickham-Jones, and C. J. S. M. Simpson, *J. Chem. Phys.* **78**, 3881 (1983).
⁷T. A. Litovitz, *J. Chem. Phys.* **26**, 469 (1957).
⁸W. M. Madigosky and T. A. Litovitz, *J. Chem. Phys.* **34**, 489 (1961).
⁹P. K. Davis and I. Oppenheim, *J. Chem. Phys.* **57**, 505 (1972).
¹⁰C. Delalande and G. M. Gale, *J. Chem. Phys.* **71**, 4804 (1979).
¹¹J. Chesnoy, *Chem. Phys.* **83**, 283 (1984).
¹²C. Delalande and G. M. Gale, *J. Chem. Phys.* **73**, 1918 (1980).
¹³J. Chesnoy and D. Ricard, *Chem. Phys.* **67**, 347 (1982).
¹⁴D. W. Chandler and G. E. Ewing, *J. Phys. Chem.* **85**, 1994 (1981).
¹⁵J. Chesnoy and G. M. Gale, *Ann. Phys. Fr.* **9**, 893 (1984).
¹⁶D. W. Oxtoby, *Annu. Rev. Phys. Chem.* **32**, 77 (1981); *Adv. Chem. Phys.* **47**, 487 (1981).
¹⁷D. J. Diestler, *Potential Energy Surfaces*, edited by K. P. Lawley (Wiley, New York, 1980).
¹⁸D. W. Chandler and G. E. Ewing, *Chem. Phys.* **54**, 241 (1981).
¹⁹D. W. Chandler and G. E. Ewing, *J. Chem. Phys.* **73**, 4904 (1980).
²⁰See, for example, W. T. Martin and E. Reissner, *Elementary Differential Equations* (Adison-Wesley, Reading, MA, 1956).
²¹R. N. Schwartz, Z. I. Slawsky, and K. F. Herzfeld, *J. Chem. Phys.* **20**, 1591 (1952).
²²J. M. Parson, P. E. Siska, and Y. T. Lee, *J. Chem. Phys.* **56**, 1511 (1972).
²³A. F. Devonshire, *Proc. R. Soc. London Ser. A* **158**, 269 (1937).
²⁴S. L. Thompson, *J. Chem. Phys.* **49**, 3400 (1968).
²⁵K. F. Herzfeld and T. A. Litovitz, *Absorption and Dispersion of Ultrasonic Waves* (Academic, New York, 1959).
²⁶J. D. Lambert, *Vibrational and Rotational Relaxation in Gases* (Oxford University, Oxford, 1977), p. 47.
²⁷J. L. Stretton, *Trans. Faraday Soc.* **61**, 1053 (1965).
²⁸G. E. Ewing (unpublished work).
²⁹A. A. Frost and R. G. Pearson, *Kinetics and Mechanism*, 2nd ed. (Wiley, New York, 1953), p. 60.
³⁰J. O. Hirschfelder, C. F. Curtis, and R. B. Bird, *The Molecular Theory of Gases and Liquids* (Wiley, New York, 1957).
³¹G. E. Ewing, *Chem. Phys.* **29**, 253 (1978).
³²D. Rapp and T. Kassal, *Chem. Rev.* **69**, 61 (1969).
³³B. H. Mahan, *J. Chem. Phys.* **46**, 98 (1962).
³⁴J. C. Stephenson, R. E. Wood, and C. B. Moore, *J. Chem. Phys.* **48**, 4790 (1968).
³⁵J. T. Yardley, *Introduction to Molecular Energy Transfer* (Academic, New York, 1980).
³⁶G. A. Kaprolova, E. E. Nikitin, and A. M. Chaikin, *Chem. Phys. Lett.* **2**, 581 (1968).
³⁷P. F. Zittel and C. B. Moore, *J. Chem. Phys.* **58**, 2004 (1973).
³⁸D. G. Jones, J. D. Lambert, and J. L. Stretton, *J. Chem. Phys.* **43**, 4541 (1965).
³⁹W. F. Calaway and G. E. Ewing, *J. Chem. Phys.* **69**, 1418 (1978).
⁴⁰P. Hess and C. B. Moore, *J. Chem. Phys.* **65**, 2339 (1976).
⁴¹E. A. Gregory, M. R. Buckingham, D. Z. Clayton, F. J. Wolfenden, and C. J. S. M. Simpson, *Chem. Phys. Lett.* **104**, 393 (1984).
⁴²C. Manzanares and G. Ewing, *J. Chem. Phys.* **69**, 1418 (1978).
⁴³A. Jeannotte II, D. Legler, and J. Overend, *Spectrochim. Acta Part A*, **29**, 1915 (1973).
⁴⁴L. Verlet, *Phys. Rev.* **165**, 201 (1968).
⁴⁵J. Chesnoy, *Chem. Phys.* **83**, 283 (1984).
⁴⁶H. C. Anderson, J. D. Weeks, and D. Chandler, *Phys. Rev. A* **4**, 1579 (1971).